Spontaneous Twisting of Achiral Hard Rod Nematics

Davide Revignas and Alberta Ferrarini[*]

Department of Chemical Sciences, University of Padova Via Marzolo 1, 35131 Padova, Italy

Since Onsager's seminal work, hard rods have been taken as a prototype of nematic liquid crystals, characterized by uniaxial order and a uniform director field as a ground state. Here, using Onsager theory to calculate the free energy in the presence of arbitrary deformations, we find that hard rod nematics have an intrinsic tendency to twist around their ordering axis (double twist), driven by a mechanism in which the orientational fluctuations of particles play a key role. The anisotropic hard core potential used here is arguably the simplest form of interaction able to originate spontaneous breaking of mirror symmetry in a 3D fluid. Our results are discussed in relation to the recent discovery of a double twisted ground state in cylindrically confined lyotropic chromonic liquid crystals.

Chirality is a hallmark of living systems, and explaining the origin of homochirality is a fundamental question [1]. Besides its relevance in biology [2], understanding and controlling the mechanisms that control the buildup of chirality in matter also has practical implications, e.g., for the rational design of materials for asymmetric catalysis [3,4] and photonic [5,6] applications. Meso- and macroscopic chiral structures in condensed matter are generally observed in systems endowed with chirality at the microscopic level, but they can also emerge from the organization of achiral building blocks. This phenomenon, denoted as spontaneous mirror symmetry breaking (SMSB) spans the fields of crystals [7], colloids [8], gels [9], supramolecular polymers [10], and liquid crystals [11], and has generally been explained as the result of the interplay of competing interparticle interactions and boundary effects. A prominent example, ubiquitous in polymer crystallization from melts, is the formation of spherulites, characterized by a concerted twisting of crystallographic orientation. The first detailed investigation on polyethylene, an achiral polymer simply made of a sequence of identical methylene groups, dates to the mid-1950s [12]. The emergence of chirality from achiral elements in fluids was thought impossible, until in the late 1990s a case was reported in smectic liquid crystals made of bent molecules [13]. Then, in the last decade achiral bent molecules were found to form the twist-bend nematic phase [14–16], where the average molecular orientation (the director $\hat{n}$) exhibits a heliconical modulation with nanoscale pitch. Indeed liquid crystals, owing to the combination of order and fluidity, have proven to be an excellent playground to explore the relationship between microscopic and higher level symmetries.

A challenging behavior was recently reported in lyotropic chromonic liquid crystals (LCLCs), biocompatible systems made of amphiphilic planklike molecules, which in water self-assemble into columnar aggregates that beyond a certain density align along a common direction. LCLCs were found to form chiral tactoids [17] and to take double twisted director configurations under confinement in cylindrical [18–20] or rectangular [21] capillaries and in cylindrical shells [22] with degenerate planar boundary conditions. This phenomenon was ascribed to unconventional elastic properties. Using a recent reformulation [23], which is convenient to our purpose, the deformation free energy density [24,25] of achiral nematic liquid crystals can be expressed as

$$\Delta a^{\text{def}} = \frac{1}{2}(K_{11} - K_{24})S^2 + \frac{1}{2}(K_{22} - K_{24})T^2 + \frac{1}{2}K_{33}B^2 + K_{24}\text{Tr}(\boldsymbol{\Delta}^2) \tag{1}$$

where $\mathbf{S} = \hat{\boldsymbol{n}}(\nabla \cdot \hat{\boldsymbol{n}})$, $T = \hat{\boldsymbol{n}} \cdot (\nabla \times \hat{\boldsymbol{n}})$, $\mathbf{B} = -(\hat{\boldsymbol{n}} \cdot \nabla)\hat{\boldsymbol{n}} = \hat{\boldsymbol{n}} \times (\nabla \times \hat{\boldsymbol{n}})$ represent the splay, twist, and bend mode, respectively, and $\boldsymbol{\Delta}$ is a fourth mode described by a second-rank tensor whose elements are defined as $\Delta_{ij} = \frac{1}{2}[\partial_i n_j + \partial_j n_i - n_i n_k \partial_k n_j - n_j n_k \partial_k n_i]$. K_{ii} ($i = 1, 2, 3$) and K_{24} are elastic constants [26]; for $K_{11} > K_{24}$, $K_{22} > K_{24}$, $K_{33} > 0$ and $K_{24} > 0$, which is the case of typical nematics, the ground state is a uniform director [27]. LCLCs would be a special case with $K_{22} < K_{24}$, hence their spontaneous tendency to twist. However this poses a major question: what is the microscopic mechanism underlying spontaneous twist in a 3D fluid of axially symmetric particles?

Here we have addressed this question considering a minimalist model of hard rods. Previous studies showed that excluded volume interactions are able to induce SMSB in condensed matter. It is well known that, for purely geometrical reasons, achiral objects, such as spheres and tetrahedra, can pack into helical structures [28]. Right- and

left-handed chiral structures were found in 2D liquid crystals of achiral hard triangles [29–32] and rodlike particles [33–35]. In a 3D fluid of rigid, achiral bent particles, excluded volume interactions, which reflect the transversal shape polarity of particles, were shown to drive the formation of the twist-bend nematic phase, characterized by local transversal polar order [36,37]. In this Letter we show that the ability to induce SMSB in a 3D fluid is encoded in an even simpler interaction, and the driving mechanism is different from the other cases mentioned so far, since a key role is played by the orientational fluctuations of particles. This result is obtained using Onsager-Straley theory [38,39] to calculate the full set of nematic elastic constants, including the saddle splay one, K_{24}. This is an achievement by itself, since K_{24}, which is believed to play a key role in relevant phenomena [40], remains a controversial quantity, mainly owing to the difficulty of its accurate experimental determination. The controversy concerns the theoretical determination of K_{24} as well [41], and this has discouraged progress in modeling.

The starting point in our microscopic approach is an expression for the Helmholtz free energy. This includes an ideal contribution, which is the sum of the ideal gas term and a term accounting for the decrease in rotational entropy due to nematic ordering, in addition to an excess contribution that originates from interparticle interactions. Under the common assumption that orientational order is not perturbed, which is valid for deformations on a length scale far above the molecular size, director distortions affect only the excess free energy. This quantity is generally expressed as a double integral of a kernel related to the pair interaction, $g(\boldsymbol{R}_A, \boldsymbol{R}_B, \hat{\boldsymbol{n}}(\boldsymbol{R}_A), \hat{\boldsymbol{n}}(\boldsymbol{R}_B))$, taken over the position of the c.m. of two particles ($\boldsymbol{R}_A$ and $\boldsymbol{R}_B$). The standard procedure consists of Taylor expanding the director in this kernel with respect to the undeformed state, and terms proportional to the square of the first derivatives are retained. The identification of the elastic constants as the coefficients of the invariants appearing in Eq. (1) involves the definition of a free energy density in the Oseen-Frank sense; an intrinsic ambiguity in this definition was pointed out [41], which would translate into an ambiguity in the microscopic definition of the so-called surfacelike elastic constants, such as K_{24}. Here, we have bypassed this problem by calculating the free energy of a finite volume. To avoid boundary effects, this is thought to be a small cubic box with virtual walls, in the interior of a large macroscopic body (see Fig. 1 and the Supplemental Material [42]). Considering a system of hard rodlike particles, the excess free energy of the small box of volume V is expressed at the second virial level [38] as

$$\frac{A^{\text{ex}}}{k_B T} = -\frac{\eta \rho^2}{2} \int_V d\boldsymbol{R}_A \int_{\mathcal{V}} d\boldsymbol{R}_B \int_{\mathbb{S}^2} d\hat{\boldsymbol{u}}_A \int_{\mathbb{S}^2} d\hat{\boldsymbol{u}}_B$$
$$\times f(\hat{\boldsymbol{u}}_A \cdot \hat{\boldsymbol{n}}(\boldsymbol{R}_A)) f(\hat{\boldsymbol{u}}_B \cdot \hat{\boldsymbol{n}}(\boldsymbol{R}_B)) e_{AB}(\boldsymbol{R}_{AB}, \hat{\boldsymbol{u}}_A, \hat{\boldsymbol{u}}_B) \quad (2)$$
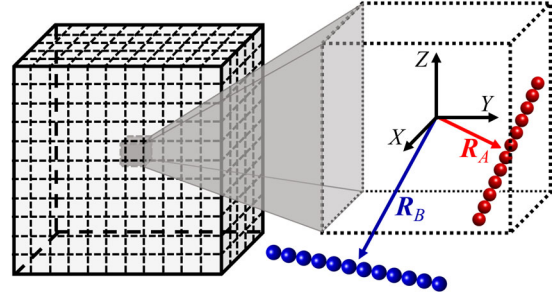

FIG. 1. Macroscopic body of volume $\mathcal{V}$ (on the left) and inner box of volume V, enclosed by virtual walls (on the right). $\boldsymbol{R}_A$ and $\boldsymbol{R}_B$ are position vectors of the c.m. of particles A and B.

where $\boldsymbol{R}_{AB} = \boldsymbol{R}_B - \boldsymbol{R}_A$, $\hat{\boldsymbol{u}}_A$, and $\hat{\boldsymbol{u}}_B$ are unit vectors parallel to the axis of the two particles, and $e_{AB}(\boldsymbol{R}_{AB}, \hat{\boldsymbol{u}}_A, \hat{\boldsymbol{u}}_B)$ is the Mayer function, defined on the basis of the interaction potential U_{AB}: $e_{AB}(\boldsymbol{R}_{AB}, \hat{\boldsymbol{u}}_A, \hat{\boldsymbol{u}}_B) = \exp\{-U_{AB}(\boldsymbol{R}_{AB}, \hat{\boldsymbol{u}}_A, \hat{\boldsymbol{u}}_B)/k_B T\} - 1$ [43]. Moreover, $\rho = N/V$, with N the number of particles in the volume V, is the number density, whereas η is the modified Parsons-Lee [44,45] factor, $\eta = (1 - 4\rho v_{\text{eff}}/3)/(1 - \rho v_{\text{eff}})^2$, with v_{eff} the *effective* volume of a single particle [46] [see the Supplemental Material for details and justification of Eq. (2)]. Finally, $f(\hat{\boldsymbol{u}} \cdot \hat{\boldsymbol{n}}(\boldsymbol{R}))$ is the single particle orientational distribution function (ODF), which in general can be thought of as a function of the angle between the axis of a rod and the local director at the position of its center of mass. The outermost integral in Eq. (2), over the position of one particle, extends to the volume V of the small box, whereas the next integral, over the coordinates of the other particle, is over the whole volume $\mathcal{V}$ of the macroscopic body.

For the connection with Oseen-Frank free energy we considered the following explicit forms of the director field:

$$\hat{\boldsymbol{n}}(\boldsymbol{R}, q) = \begin{cases} [qX, 0, (1+qZ)](q^2 X^2 + (1+qZ)^2)^{-1/2} \\ [\sin(qY), 0, \cos(qY)] \\ [qZ, 0, (1-qX)](q^2 Z^2 + (1-qX)^2)^{-1/2} \quad (3) \\ [qX, -qY, 1](1 + q^2(X^2 + Y^2))^{-1/2} \\ [-qY, qX, 1](1 + q^2(X^2 + Y^2))^{-1/2} \end{cases}$$

where q plays the role of deformation wavelength. For $q \to 0$ these deformations correspond to approximately pure splay, twist, bend, Δ mode and double twist, respectively; thus the integral of Eq. (1) over a cubic box of volume V in the presence of such deformations in the regime $qV^{1/3} \ll 1$ gives

$$\Delta A^{\text{def}}(q) \simeq \begin{cases} \frac{1}{2} q^2 \ V \ K_{11} \\ \frac{1}{2} q^2 \ V \ K_{22} \\ \frac{1}{2} q^2 \ V \ K_{33} \quad (4) \\ 2q^2 \ V \ K_{24} \\ 2q^2 \ V \ (K_{22} - K_{24}). \end{cases}$$

It can be noted that K_{24} is treated on the same footing of the other three (often dubbed "bulk") elastic constants; the fifth deformation, which locally corresponds to pure double twist, does not add new information, but is used here as a consistency check. Based on Eq. (4), the elastic constants are obtained by parabolic fitting of the microscopic deformation free energy calculated for the director fields defined in Eq. (3). It may be worth mentioning that the method can be extended to any arbitrary deformation, the only limit being the assumption of constant order parameter, which might fail for short range deformations.

We performed calculations for rigid linear chains of M tangent hard spheres of diameter σ, with the interaction potential defined as $U_{AB} = \infty$ if at least two spheres overlap; otherwise $U_{AB} = 0$. For the ODF we adopted the simplest form compatible with local $\mathcal{D}_{\infty h}$ symmetry: $f(\hat{\boldsymbol{u}} \cdot \hat{\boldsymbol{n}}(\boldsymbol{R})) = \exp\{c[\hat{\boldsymbol{u}} \cdot \hat{\boldsymbol{n}}(\boldsymbol{R})]^2\}/\int_{\mathbb{S}^2} d\hat{\boldsymbol{u}} \exp\{c[\hat{\boldsymbol{u}} \cdot \hat{\boldsymbol{n}}(\boldsymbol{R})]^2\}$, where c is a parameter related to the nematic order parameter S. Given the number density ρ, or the volume fraction $\phi = v_0\rho$, where v_0 is the geometrical volume of a single particle, the equilibrium value of c is determined by minimization [47] of the total Helmholtz free energy in the undeformed nematic phase (see Ref. [48] and the Supplemental Material for details). All results reported in the following were obtained for linear chains of $M = 12$ spheres at $\phi = 0.21$ ($S = 0.79$), slightly above the isotropic-nematic transition.

Figure 2 shows the deformation free energy $\Delta A^{\mathrm{def}}(q) = A^{\mathrm{ex}}(q) - A^{\mathrm{ex}}(q=0)$, together with the results of parabolic fitting according to Eq. (4). The bulk elastic constants are in the order $K_{33} > K_{11} > K_{22}$, as already found for hard rodlike particles [49]; what is interesting is that K_{24} is higher than all the other constants but K_{33}. Accordingly, the deformation free energy for double twist has negative curvature, which indicates a spontaneous tendency to double twist. Although hard particle models can be used to describe the behavior of lyotropic liquid crystals [38,50] a strict comparison with experimental values for LCLCs is not possible since these are multicomponent systems, made of multidisperse columnar aggregates, which cannot be simply mapped into a collection of identical rigid rods. Anyway, we may notice that estimates of the bulk elastic constants based on the values in Fig. 2, with $\sigma \sim 1$ nm [51], have the same magnitude and relative order as experimental data for Sunset Yellow, a typical LCLC with a persistence length of about 10 nm ($K_{11} = 4.3$ pN, $K_{22} = 0.7$ pN, $K_{33} = 6.1$ pN, at T around 300 K and $\phi = 0.20$) [52]. For K_{24} two quite different values can be found in the literature, that is 27.5 pN [18] and 6.25 pN [53], of which the latter compares well with our prediction.

According to Onsager theory, what drives the formation of the uniaxial nematic phase is the decrease of excluded volume ongoing from an isotropic to a uniaxial orientational distribution of particles. However, there is a more subtle effect, which comes from orientational fluctuations:
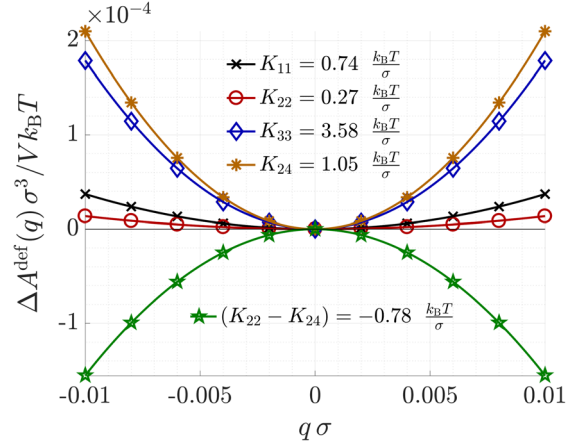

FIG. 2. Deformation free energy ΔA^{def} as a function of the deformation wave number q, for the modes defined in Eq. (3). Lines show the results of parabolic fitting to Eq. (4).

the excluded volume between two rods with some degree of orientational disorder is smaller when they slide on each other with a preferential twist, rather than keeping, on average, a parallel configuration. This can be clearly appreciated in the contour plot in Fig. 3(a), which shows the difference of the average excluded volume in double twist [defined as in Eq. (3)] and in uniform director field ($\hat{\boldsymbol{n}} \| Z$), for a rod having its c.m. on the XZ plane, which rotates around a rod with its c.m. in the origin. Here we can see that the largest contribution comes from side-by-side configurations where the centers of mass of the rods are close to each other. The mechanism underlying spontaneous twist is illustrated by the cartoons in Figs. 3(b)–3(c), where hourglasses mimic the volume occupied by a rod that fluctuates around its main ordering axis. We can conjecture that the very same mechanism will also contribute spontaneous twisting of hard rods in 2D [35].

From a first glance at Fig. 2 one could guess that double twist corresponds to a free energy unbounded from below. Actually, owing to compatibility constraints, double twist in 3D Euclidean space is necessarily accompanied by other deformation modes, whose cost prevents the free energy from going to negative infinity [54]. Let us consider a double twist configuration in a cylinder of radius R_{max} and height h, with free boundary conditions on the surface. Assuming the director field $\hat{\boldsymbol{n}}(r) = [0, \sin\theta(r), \cos\theta(r)]$ in cylindrical coordinates [54] where $\theta(r)$ is the twist angle, integration of Eq. (1) leads to the following expression for the deformation free energy per unit length:

$$\frac{\Delta A^{\mathrm{def}}[\theta(r)]}{h} = 2\pi \int_0^{R_{\mathrm{max}}} dr\, r \left\{ \frac{K_{24}}{2}\left(\theta' - \frac{\sin(2\theta)}{2r}\right)^2 \right.$$
$$\left. + K_{33}\frac{\sin^4\theta}{2r^2} + \frac{1}{2}(K_{22} - K_{24})\left(\theta' + \frac{\sin(2\theta)}{2r}\right)^2 \right\}$$
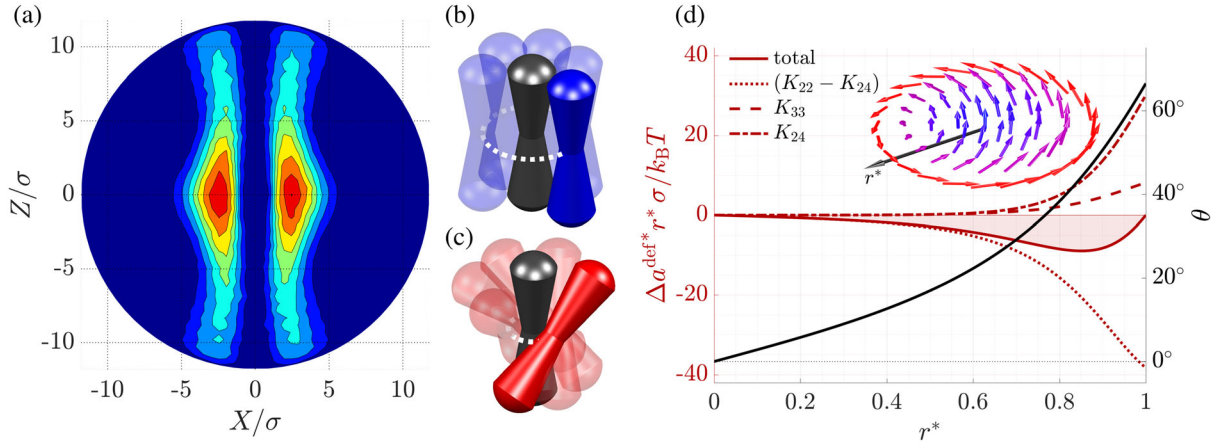
$$(5)$$

FIG. 3. (a) Contour plot of the difference between average excluded volume in double twist and in uniform director field, for two rods having their c.m. in the origin and in the XZ plane, respectively. The director field is defined as in Eq. (3) with $q = 0.05\sigma^{-1}$ in double twist, whereas it is parallel to the Z axis in the uniform system. Color ranges from blue to red for increasingly negative values. Cartoons illustrating the excluded volume between pairs of particles in (b) a uniform and (c) a double twist director field. Hourglasses represent the volume occupied by a rod fluctuating around its ordering axis. (d) Twist angle θ (black solid line) along with the profile of the scaled deformation free energy density $\Delta a^{\mathrm{def}^*} = \Delta a^{\mathrm{def}} R_{\mathrm{max}}^2$ (red solid line) and the contribution of different modes according to Eq. (5) (dashed lines), as a function of the reduced radius $r^* = r/R_{\mathrm{max}}$. Inset: double twist configuration, with arrows representing the director field, $\hat{\boldsymbol{n}}(r^*) = [0, \sin\theta(r^*), \cos\theta(r^*)]$.

where $\theta' = d\theta(r)/dr$. The profile of $\theta(r)$ that minimizes the free energy is determined by the competition between the tendency to double twist and the restoring force opposing the simultaneous bend and Δ deformations. It is obtained by solving the corresponding Euler-Lagrange equation with $\theta(0) = 0$ and free boundary condition at $r = R_{\mathrm{max}}$ (see the Supplemental Material [42] for details). The black line in the plot in Fig. 3(d) shows the numerical solution [55], calculated using the elastic constants reported in Fig. 2, as a function of the reduced radius $r^* = r/R_{\mathrm{max}}$. The twist angle reaches a value of around 65° at the boundary, with a slope that increases with the scaled distance from the cylinder axis. Positive θ values correspond to a right-handed twist; however, given the symmetry of Eq. (5) with respect to a change of sign of the twist angle, there is an equivalent degenerate solution corresponding to a left-handed twist. The presence of chirality in particles would yield an additional linear twist term in the deformation free energy, with the primary effect of making inequivalent the two solutions. The plot in Fig. 3(d) also reports the profiles of the scaled deformation free energy density and of the contributions of different modes [see Eq. (5)] multiplied by r^* so that the area under the curves is a deformation free energy per unit length. We can see that, as a consequence of the high value of K_{24}, the tendency to twist is counterbalanced by a large cost of Δ mode, which adds to a smaller contribution for bending.

Experimental evidence of spontaneous double twist has been reported for confined achiral LCLCs [18–22], and this has created interest in what would be unique in these systems. Actually, our results point to an entropically driven mechanism, which would be quite general for rodlike lyotropic liquid crystals; this suggests extending the experimental investigation to other achiral lyotropic systems [56]. Whether spontaneous twist can be expected in thermotropic liquid crystals, which are typically made of relatively flexible molecules with a role of attractive dispersion interactions, deserves further investigation. Interestingly, transient twisted defect structures were recently reported in achiral thermotropic nematics [57], but at present it is hard to say if there is a relation with our findings.

Double twist structures are typical of liquid crystal blue phases [58] and half-skyrmions [59], both observed in chiral materials, so their existence has been commonly discussed in terms of molecular chirality. Here we have shown that an intrinsic tendency toward double twist is encoded in uniaxial nematic order driven by excluded volume interactions between rigid uniaxial particles. Instability of uniform uniaxial order leads to SMSB, and finite twist is achieved only because of the elastic cost for other accompanying deformations. This mechanism is quite different from that underlying cholesteric order (twist along a direction perpendicular to the ordering axis), which requires molecular chirality and corresponds to a stable thermodynamic state. An analogous scenario was proposed to distinguish self-limiting assembly in twisted bundles of chiral and achiral systems [60], although in that case fluctuations were frozen and a possible driving force for spontaneous twist was identified in the cohesive interactions between semiflexible filaments.

In summary, we report on a distinct entropic mechanism for SMSB in rodlike nematics, with a special role of orientational fluctuations leading to an elastic instability.

Hopefully this will serve to stimulate experimental and theoretical work, to further explore the existence of similar mechanisms in soft matter, where chiral structures are involved in phenomena as diverse as the creation of topological states [61] or the organization of biofilaments in cells [62,63].

---

*Corresponding author.
alberta.ferrarini@unipd.it

[1] A. Guijarro and M. Yus, *The Origin of Molecular Chirality in the Molecules of Life* (RSC, Cambridge, 2009).

[2] M. Novak, B. Polak, J. Simunic, Z. Boban, B. Kuzmic, A. W. Thomae, I. M. Tolic, and N. Pavin, The mitotic spindle is chiral due to torques within microtubule bundles, Nat. Commun. **9**, 3571 (2018).

[3] R. E. Morris and X. Bu, Induction of chiral porous solids containing only achiral building blocks, Nat. Chem. **2**, 353 (2010).

[4] H. Zhang, S. Li, A. Qu, C. Hao, M. Sun, L. Xu, C. Xu, and H. Kuang, Engineering of chiral nanomaterials for biomimetic catalysis, Chem. Sci. **11**, 12937 (2020).

[5] J. B. Pendry, A chiral route to negative refraction, Science **306**, 1353 (2004).

[6] E. Plum, V. A. Fedotov, and N. I. Zheludev, Optical activity in extrinsically chiral metamaterial, Appl. Phys. Lett. **93**, 191911 (2008).

[7] C. Li, A. G. Shtukenberg, L. Vogt-Maranto, P. R. Efi Efrati, J. D. Gale, A. L. Rohl, and B. Kahr, Why are some crystals straight?, J. Phys. Chem. C **124**, 15616 (2020).

[8] Y. Yin and Y. Xia, Self-assembly of spherical colloids into helical chains with well-controlled handedness, J. Am. Chem. Soc. **125**, 2048 (2003).

[9] C. D. Jones, H. T. D. Simmons, K. E. Horner, K. Liu, R. L. Thompson, and J. W. Steed, Braiding, branching and chiral amplification of nanofibres in supramolecular gels, Nat. Chem. **11**, 375 (2019).

[10] G. B. Schuster, B. J. Cafferty, S. C. Karunakaran, and N. V. Hud, Water-soluble supramolecular polymers of paired and stacked heterocycles: Assembly, structure, properties, and a possible path to pre-RNA, J. Am. Chem. Soc. **143**, 9279 (2021).

[11] C. Tschierske, Chiral shape fluctuations and the origin of chirality in cholesteric phases of DNA origamis, Liq. Cryst. **45**, 2221 (2018).

[12] A. Keller, The spherulitic structure of crystalline polymers. Part I. Investigations with the polarizing microscope, J. Polym. Sci. **17**, 291 (1955).

[13] D. R. Link, G. Natale, R. Shao, J. E. Maclennan, N. A. Clark, E. Korblova, and D. M. Walba, Spontaneous formation of macroscopic chiral domains in a fluid smectic phase of achiral molecules, Science **278**, 1924 (1997).

[14] M. Cestari, E. Frezza, A. Ferrarini, and G. R. Luckhurst, Crucial role of molecular curvature for the bend elastic and exoelectric properties of liquid crystals: Mesogenic dimers as a case study, J. Mater. Chem. **21**, 12303 (2011).

[15] V. Borshch, Y.-K. Kim, J. Xiang, M. Gao, A. Jakli, V. P. Panov, J. K. Vij, C. T. Imrie, M. G. Tamba, G. H. Mehl, and O. D. Lavrentovich, Nematic twist-bend phase with nanoscale modulation of molecular orientation, Nat. Commun. **4**, 2635 (2013).

[16] D. Chen, J. H. Porada, J. B. Hooper, A. Klittnick, Y. Shen, M. R. Tuchband, E. Korblova, D. Bedrov, D. M. Walba, M. A. Glaser, J. E. Maclennan, and N. A. Clark, Chiral heliconical ground state of nanoscale pitch in a nematic liquid crystal of achiral molecular dimers, Proc. Natl. Acad. Sci. U.S.A. **110**, 15931 (2013).

[17] L. Tortora and O. D. Lavrentovich, Chiral symmetry breaking by spatial confinement in tactoidal droplets of lyotropic chromonic liquid crystals, Proc. Natl. Acad. Sci. U.S.A. **108**, 5163 (2011).

[18] Z. S. Davidson, L. Kang, J. Jeong, T. Still, P. J. Collings, T. C. Lubensky, and A. G. Yodh, Chiral structures and defects of lyotropic chromonic liquid crystals induced by saddle-splay elasticity, Phys. Rev. E **91**, 050501(R) (2015).

[19] K. Nayani, R. Chang, J. Fu, P. W. Ellis, A. Fernandez-Nieves, J. O. Park, and M. Srinivasarao, Spontaneous emergence of chirality in achiral lyotropic chromonic liquid crystals confined to cylinders, Nat. Commun. **6**, 8067 (2015).

[20] J. Eun, S.-J. Kim, and J. Jeong, Effects of chiral dopants on double-twist configurations of lyotropic chromonic liquid crystals in a cylindrical cavity, Phys. Rev. E **100**, 012702 (2019).

[21] J. Fu, K. Nayani, J. O. Park, and M. Srinivasarao, Spontaneous emergence of twist and the formation of a monodomain in lyotropic chromonic liquid crystals confined to capillaries, NPG Asia Mater. **9**, e393 (2017).

[22] A. Javadi, J. Eun, and J. Jeong, Cylindrical nematic liquid crystal shell: effect of saddle-splay elasticity, Soft Matter **14**, 9005 (2018).

[23] J. V. Selinger, Interpretation of saddle-splay and the Oseen-Frank free energy in liquid crystals, Liq. Cryst. Rev. **6**, 129 (2018).

[24] C. W. Oseen, The theory of liquid crystals, Trans. Faraday Soc. **29**, 883 (1933).

[25] F. C. Frank, I. Liquid crystals. On the theory of liquid crystals, Discuss. Faraday Soc. **25**, 19 (1958).

[26] In comparing K_{24} values from different sources, attention must be paid to the form of the saddle-splay contribution in the expression used for Oseen-Frank free energy. Here, data taken from different sources were converted, when needed, to be consistent with the form of Eq. (1).

[27] J. L. Ericksen, Inequalities in liquid crystal theory, Phys. Fluids **9**, 1205 (1966).

[28] G. T. Pickett, M. Gross, and H. Okuyama, Spontaneous Chirality in Simple Systems, Phys. Rev. Lett. **85**, 3652 (2000).

[29] K. Zhao, R. Bruinsma, and T. G. Mason, Local chiral symmetry breaking in triatic liquid crystals, Nat. Commun. **26,** 152101 (2013).

[30] S. P. Charmichael and M. S. Shell, A simple mechanism for emergent chirality in achiral hard particle assembly, J. Chem. Phys. **139,** 164705 (2013).

[31] A. P. G. W. Qiab and M. Dijkstra, A novel chiral phase of achiral hard triangles and an entropy-driven demixing of enantiomers, Soft Matter **11,** 8684 (2015).

[32] N. Pakalidou, D. L. Cheung, A. J. Masters, and C. Avendano, Macroscopic chiral symmetry breaking in mono-layers of achiral nonconvex platelets, Soft Matter **13,** 8618 (2017).

[33] L. Kang, T. Gibaud, Z. Dogic, and T. C. Lubensky, Entropic forces stabilize diverse emergent structures in colloidal membranes, Soft Matter **12,** 386 (2016).

[34] X. Liu, Z. Chen, Q. Liu, G. H. Sheetah, N. Sun, P. Zhao, Y. Xie, and I. I. Smalyukh, Morphological and orientational controls of self-assembly of gold nanorods directed by evaporative microflows, ACS Appl. Mater. Interfaces **13,** 53143 (2021).

[35] Z. Kost-Smith, Emergent phenomena in minimal models of soft matter, Ph.D. thesis, B. A., Colorado School of Mines, 2014.

[36] C. Greco and A. Ferrarini, Entropy-Driven Chiral Order in a System of Achiral Bent Particles, Phys. Rev. Lett. **115,** 147801 (2015).

[37] M. Chiappini, T. Drwenski, R. van Roij, and M. Dijkstra, Biaxial, Twist-Bend, and Splay-Bend Nematic Phases of Banana-Shaped Particles Revealed by Lifting the "Smectic Blanket", Phys. Rev. Lett. **123,** 068001 (2019).

[38] L. Onsager, The effects of shape on the interaction of colloidal particles, Ann. N.Y. Acad. Sci. **51,** 627 (1949).

[39] J. Straley, Frank elastic constants of the hard-rod liquid crystal, Phys. Rev. A **8,** 2181 (1973).

[40] Z. Kos and M. Ravnik, Relevance of saddle-splay elasticity in complex nematic geometries, Soft Matter **12,** 1313 (2016).

[41] A. M. Somoza and P. Tarazona, Density functional theory of the elastic constants of a nematic liquid crystal, Mol. Phys. **72,** 911 (1991).

[42] See Supplemental Material at http://link.aps.org/supplemental/10.1103/PhysRevLett.130.028102 for theoretical and computational details.

[43] C. Gray and K. E. Gubbins, *Theory of Molecular Fluids: Volume 1: Fundamentals* (Oxford University Press, New York, 1984).

[44] J. D. Parsons, Nematic ordering in a system of rods, Phys. Rev. A **19,** 1225 (1979).

[45] S.-D. Lee, A numerical investigation of nematic ordering based on a simple hard-rod model, J. Chem. Phys. **87,** 4972 (1987).

[46] S. Varga and I. Szalai, Modified Parsons-Lee theory for fluids of linear fused hard sphere chains, Mol. Phys. **98,** 693 (2000).

[47] J. C. Lagarias, J. A. Reeds, M. H. Wright, and P. E. Wright, Convergence properties of the Nelder–Mead simplex method in low dimensions, SIAM J. Optim. **9,** 112 (1998).

[48] D. Revignas and A. Ferrarini, Microscopic modelling of nematic elastic constants beyond Straley theory, Soft Matter **18,** 648 (2022).

[49] S.-D. Lee, Density-functional approach to curvature elasticity in a liquid-density nematic system, Phys. Rev. A **39,** 3631 (1989).

[50] L. Mederos, E. Velasco, and Y. Martinez-Raton, Hard-body models of bulk liquid crystals, J. Phys. Condens. Matter **26,** 463101 (2014).

[51] D. J. Edwards, J. W. Jones, O. Lozman, A. P. Ormerod, M. Sintyureva, and G. J. T. Tiddy, Chromonic liquid crystal formation by edicol sunset yellow, J. Chem. Phys. **112,** 14628 (2008).

[52] S. Zhou, Y. A. Nastishin, M. M. Omelchenko, L. Tortora, V. G. Nazarenko, O. P. Boiko, T. Ostapenko, T. Hu, C. C. Almasan, S. N. Sprunt, J. T. Gleeson, and O. D. Lavrentovich, Elasticity of Lyotropic Chromonic Liquid Crystals Probed by Director Reorientation in a Magnetic Field, Phys. Rev. Lett. **109,** 037801 (2012).

[53] T. C. Lubensky, Confined chromonics and viral membranes, Mol. Cryst. Liq. Cryst. **646,** 235 (2017).

[54] C. Long and J. V. Selinger, Violation of Ericksen inequalities in lyotropic chromonic liquid crystals, J. Elast. 1 (2022).

[55] W. Auzinger, G. Kneisl, O. Koch, and E. Weinmüller, A collocation code for singular boundary value problems in ordinary differential equations, Numer. Algorithms, **33,** 27 (2003).

[56] After submission of this manuscript we learned that a double twisted director configuration was recently found in a cylindrically confined racemic mixture of poly-γ-benzyl-L- and D-glutamate (M. Srinivasarao *et al.*, Emergence of chirality in achiral systems, *International Liquid Crystal Conference ILCC2022, Lisbon, July 2022*).

[57] J. X. Velez, Z. Zheng, D. A. Beller, and F. Serra, Emergence and stabilization of transient twisted defect structures in confined achiral liquid crystals at a phase transition, Soft Matter **17,** 3848 (2021).

[58] D. C. Wright and N. D. Mermin, Crystalline liquids: the blue phases, Rev. Mod. Phys. **61,** 385 (1989).

[59] A. Nych, J. Fukuda, U. Ognysta, S. Zumer, and I. Musevic, Spontaneous formation and dynamics of half-skyrmions in a chiral liquid-crystal film, Nat. Phys. **13,** 1215 (2017).

[60] G. M. Grason, Chiral and achiral mechanisms of self-limiting assembly of twisted bundles, Soft Matter **16,** 1102 (2020).

[61] I. Smalyukh, Review: knots and other new topological effects in liquid crystals and colloids, Rep. Prog. Phys. **83,** 106601 (2020).

[62] Y. H. Tee, T. Shemesh, V. Thiagarajan, R. F. Hariadi, K. L. Anderson, C. Page, N. Volkmann, D. Hanein, S. Sivaramakrishnan, M. M. Kozlov, and A. D. Bershadsky, Cellular chirality arising from the self-organization of the actin cytoskeleton, Nat. Cell Biol. **17,** 445 (2015).

[63] N. Ierushalmi and K. Keren, Cytoskeletal symmetry breaking in animal cells, Curr. Opin. Cell Biol. **72,** 91 (2021).